Stereochemistry of Aldols: Configuration and Conformation of Aldols Derived from Cycloalkanones and Aldehydes

Masato Kitamura,* Keiji Nakano, Takashi Miki, Masato Okada, and Ryoji Noyori*

Contribution from the Department of Chemistry and Research Center for Materials Science, Nagoya University, Chikusa, Nagoya 464-8602, Japan

Received April 30, 2001

Abstract: The structures of cycloalkanone-based threo and erythro aldols were investigated by systematic introduction of stereo-determining factors. The combination of single-crystal X-ray analysis and cryoscopic measurement and solution NMR and IR studies elucidated the detailed geometry of these typical aldols. Currently, X-ray diffraction is the only reliable spectroscopic method to determine the relative configuration of aldols. Empirical NMR analysis can be safely applied in only limited cases. In hydrocarbon solvents, many aldols exist as monomers with an intramolecular OH···O═C hydrogen bond, but some compounds are in an equilibrium with higher aggregates via intermolecular hydrogen bonds. The aldols take various staggered conformers, where the relative stabilities are controlled largely by torsional strain affected by the size and nature of substituents. The intramolecular and intermolecular hydrogen bonds, gauche interactions between the vicinal substituents, and sometimes CH/π attractions significantly influence the distribution of conformers. The preferred structure in solution often differs greatly from the crystalline-state geometry.

Introduction

Aldol is the generic name for β-hydroxy carbonyl compounds. Threo and erythro[1] (or anti and syn[2]) diastereomers are possible when the compound possesses two consecutive stereogenic carbons at the α and β positions. These stereoisomers are selectively produced by many fundamental organic reactions, such as the aldol reaction of ketones and aldehydes,[3] reduction of α-substituted β-keto carbonyl compounds,[4] and nucleophilic ring opening of α,β-epoxy carbonyl compounds.[5] This grouping is widely found in organic compounds that show a range of biological, chemical, and physical functions.[6] In addition, aldols are useful in synthetic chemistry, because their structural characteristics allow various transformations via functional group modifications and carbon−carbon bond-forming reactions.[7,8a] The threo/erythro relative configuration, coupled with steric and electronic properties of the α and β substituents and the intramolecular or intermolecular hydrogen bond between the hydroxy hydrogen and carbonyl oxygen, strongly affects the conformation of aldols as well as the mode of intermolecular interaction. Such features further exert a significant effect on the nature and degree of the functions of aldol compounds and their assembly or complexes.

(1) (a) Noyori, R.; Nishida, I.; Sakata, J. *J. Am. Chem. Soc.* **1981**, *103*, 2106−2108. (b) Noyori, R.; Nishida, I.; Sakata, J. *J. Am. Chem. Soc.* **1983**, *105*, 1598−1608. This unambiguous terminology accommodates mostly the conventional aldol naming and is also applicable to the system in which selection of the skeletal backbone is difficult. The threo and erythro diastereomers correspond to the anti and syn isomers, respectively.[2]

(2) (a) Masamune, S.; Ali, S. A.; Snitman, D. L.; Garvey, D. S. *Angew. Chem., Int. Ed. Engl.* **1980**, *19*, 557−558. (b) Masamune, S.; Kaiho, T.; Garvey, D. S. *J. Am. Chem. Soc.* **1982**, *104*, 5521−5523.

(3) (a) Machajewski, T. D.; Wong, C.-H. *Angew. Chem., Int. Ed.* **2000**, *39*, 1352−1374. (b) Denmark, S. E.; Stavenger, R. A. *Acc. Chem. Res.* **2000**, *33*, 432−440. (c) Saito, S.; Yamamoto, H. *Chem.−Eur. J.* **1999**, *5*, 1959−1962. (d) Heathcock, C. H. The Aldol Reaction: Acid and General Base Catalysis. In *Comprehensive Organic Synthesis*; Trost, B. M., Fleming, I., Eds.; Pergamon Press: Oxford, 1991; Vol. 2, pp 133−179. (e) Heathcock, C. H. The Aldol Reaction: Group I and Group II Enolates. In *Comprehensive Organic Synthesis*; Trost, B. M., Fleming, I., Eds.; Pergamon Press: Oxford, 1991; Vol. 2, pp 181−238. (f) Kim, B. M.; Williams, S. F.; Masamune, S. The Aldol Reaction: Group III Enolates. In *Comprehensive Organic Synthesis*; Trost, B. M., Fleming, I., Eds.; Pergamon Press: Oxford, 1991; Vol. 2, pp 239−275. (g) Rathke, M. W.; Weipert, P. Zinc Enolates: The Reformatsky and Blaise Reactions. In *Comprehensive Organic Synthesis*; Trost, B. M., Fleming, I., Eds.; Pergamon Press: Oxford, 1991; Vol. 2, pp 277−299. (h) Paterson, I. The Aldol Reaction: Transition Metal Enolates. In *Comprehensive Organic Synthesis*; Trost, B. M., Fleming, I., Eds.; Pergamon Press: Oxford, 1991; Vol. 2, pp 301−319. (i) Evans, D. A.; Nelson, J. V.; Taber, T. R. In *Topics in Stereochemistry*; Eliel, E. L., Wilen, S. H., Eds.; Wiley-Interscience: New York, 1982; Vol. 13, pp 1−115. (j) Heathcock, C. H. In *Asymmetric Synthesis*; Morrison, J. D., Ed.; Academic Press: New York, 1984; Vol. 3, Chapter 2.

(4) Greeves, N. In *Comprehensive Organic Synthesis*; Trost, B. M., Fleming, I., Eds.; Pergamon Press: Oxford, 1991; Vol. 8, pp 1−24. Noyori, R. *Asymmetric Catalysis in Organic Synthesis*; John Wiley & Sons: New York, 1994; pp 56−82.

(5) Tanner, D.; Sellien, M.; Blackvall, J.-E. *J. Org. Chem.* **1989**, *54*, 3374−3378.

(6) Biologically active compounds: Fujii, I. In *Comprehensive Natural Product Chemistry*; Barton, D., Nakanishi, K., Meth-Cohn, O., Eds.; Elsevier: Oxford, U.K., 1999; Vol. 1, p 424. Richardson, M.; Khosla, C. In *Comprehensive Natural Product Chemistry*; Barton, D., Nakanishi, K., Meth-Cohn, O., Eds.; Elsevier: Oxford, U.K., 1999; Vol. 1, p 482. Staunton, J.; Wilkinson, B. In *Comprehensive Natural Product Chemistry*; Barton, D., Nakanishi, K., Meth-Cohn, O., Eds.; Elsevier: Oxford, U.K., 1999; Vol. 1, pp 495−532. MacMillan, J.; Beale, M. H. In *Comprehensive Natural Product Chemistry*; Barton, D., Nakanishi, K., Meth-Cohn, O., Eds.; Elsevier: Oxford, U.K., 1999; Vol. 2, pp 220−223. Gates, K. S. In *Comprehensive Natural Product Chemistry*; Barton, D., Nakanishi, K., Meth-Cohn, O., Eds.; Elsevier: Oxford, U.K., 1999; Vol. 7, pp 507−508. Xi, Z.; Goldberg, I. H. In *Comprehensive Natural Product Chemistry*; Barton, D., Nakanishi, K., Meth-Cohn, O., Eds.; Elsevier: Oxford, U.K., 1999; Vol. 7, pp 568−571. Chemical function: Ashmann, S. M.; Arey, J.; Atkinson, R. *J. Phys. Chem. A* **2000**, *104*, 3998−4003. Physical function: Watanabe, H.; Seto, N. *Jpn. Kokai Tokkyo Koho* **1989**, JP01318953.

(7) (a) Masamune, S.; Choy, W.; Petersen, J. S.; Sita, L. R. *Angew. Chem., Int. Ed. Engl.* **1985**, *24*, 1−30. (b) Hoffmann, R. W. *Angew. Chem., Int. Ed. Engl.* **1987**, *26*, 489−503. (c) Martin, S. F.; Lee, W.-C.; Pacofsky, G. J.; Gist, R. P.; Mulhern, T. A. *J. Am. Chem. Soc.* **1994**, *116*, 4674−4688. (d) Peterson, I.; Norcross, R. D.; Ward, R. A.; Romea, P.; Lister, M. A. *J. Am. Chem. Soc.* **1994**, *116*, 11287−11314.

10.1021/ja0110978 CCC: $20.00
Published on Web 08/24/2001

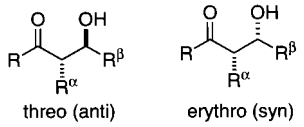

Background and General Consideration

The determination of the relative configuration of aldols, either threo or erythro, has long been a problem. Although X-ray crystallographic analysis[8] and chemical correlation are the most reliable methods, the assignment is often made by the ^{1}H NMR method that was first postulated by Stiles in 1964[9] and later extended by House (Stiles−House method).[10] This empirical rule assumes the formation of intramolecularly hydrogen-bonded six-membered structures as shown in Figure 1. The threo isomer exists in a conformational equilibrium between T_{ap} and T_{+sc}, in which the H^{α}/H^{β} relationship is antiperiplanar and (+)-synclinal, respectively. In the erythro isomer, each of the two conformers, E_{+sc} and E_{-sc}, has a (+/−)-synclinal H^{α}/H^{β} relationship. Stiles originally and cautiously stated that, if both diastereomers are monomeric with an intramolecular OH···O═C hydrogen bond (confirmed by IR in a dilute solution) and the difference in the vicinal coupling constant, $J_{\alpha,\beta}$, is distinct, namely, ∼2 Hz (erythro) versus large (threo), then the NMR method can be safely used for the determination of relative configurations. Later, considering, for some unclear reason, that the α and β substituents prefer the equatorial orientation in an imaginary chairlike conformation with respect to the hydrogen-bonded H−O−C−C−C═O six-membered system,[11,12] House postulated that threo aldols possess $J_{\alpha,\beta}$ values of 6−9 Hz and erythro isomers show values of 2−4 Hz. This method, in fact, was frequently used for the structural determination of cross aldol products. However, many examples were found for open-chain aldols which did not fit this empirical rule.[13] Sometimes the method was used rather arbitrarily without precaution, for example, without confirming the intramolecular hydrogen bond, resulting in serious misassignments. Gaudemer,[14] Evans,[3i] and

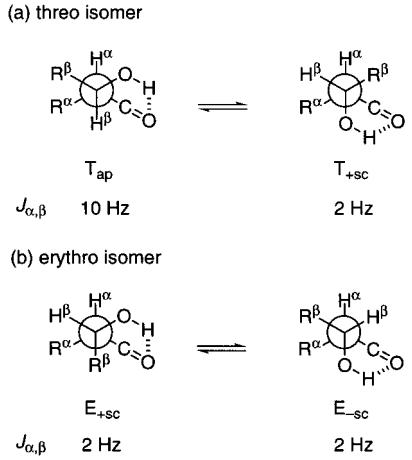

Figure 1. Hydrogen-bonded conformations of (a) threo and (b) erythro aldols. In both diastereomers, the carbonyl substituents are omitted for convenience.

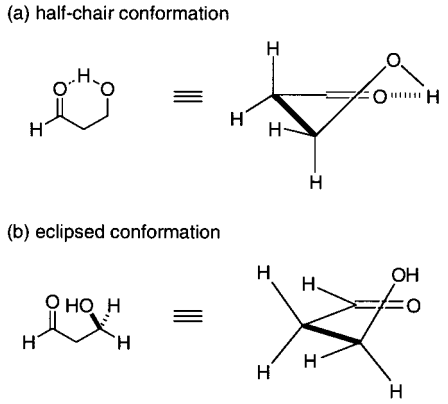

Figure 2. Possible conformations of 3-hydroxypropanal.

Heathcock[3j] advised that the Stiles−House method should be carefully used for aldols having a bulky substituent at the β position, where the enhanced gauche interaction destabilizes the hydrogen-bonded six-membered ring. Furthermore, the formation of intermolecular hydrogen bonds likely causes a conformational change which makes the NMR structural assignment difficult.

The configuration of aldols is related to their conformation. Carbonyl compounds are considered to form a hydrogen bond in the C═O plane along the direction of the sp^2 lone pairs of the oxygen atom, although the Cambridge Structural Database shows a rather broad distribution.[15] On the basis of this tendency, flexible hydrogen-bonded aldols are often depicted by a half-chair conformation. Figure 2a shows the putative geometry of the simplest aldol, 3-hydroxypropanal, which is characterized by the in-plane hydrogen bond and a staggered conformation, with respect to the α and β sp^3 carbons. However, this formulation is not appropriate. Instead, the geometry of skeletally unrestricted aldols approximates an "eclipsed" conformation, regardless of the presence or absence of a hydrogen bond. Figure 2b illustrates the structure of 3-hydroxypropanal, which possesses, among other relationships, a *syn*-C═O/OH relationship and a C(α)−C(β) linkage coplanar with the C═O plane. The C(α)/C(β) unit has a staggered conformation, while the OH proton is out of the C═O plane.

(8) (a) Yoshikawa, N.; Yamada, Y. M. A.; Sasai, H.; Shibasaki, M. *J. Am. Chem. Soc.* **1999**, *121*, 4168−4178. (b) Kutulya, L. A.; Vashchenko, V. V.; Shishkin, O. V.; Drushlyak, T. G. *Izv. Akad. Nauk, Ser. Khim.* **1998**, 2251−2257. (c) Chughtai, J. H.; Gardiner, J. M.; Harris, S. G.; Parsons, S.; Rankin, D. W. H.; Schwalbe, C. H. *Tetrahedron Lett.* **1997**, *38*, 9043−9046. (d) Kutulya, L. A.; Patsenker, L. D.; Vashchenko, V. V.; Kuznetsov, V. P.; Kulishov, V. I.; Surov, Y. N.; Kravets, V. V. *Izv. Akad. Nauk, Ser. Khim.* **1995**, 1247−1255. (e) Kutulya, L. A.; Vashchenko, V. V.; Kuznetsov, V. P.; Lakin, E. E. *Zh. Strukt. Khim.* **1994**, *35*, 133−135. (f) Schwerdtfeger, A. E.; Chan, T. H.; Thomas, A. W.; Strunz, G. M.; Salonius, A.; Chiasson, M. *Can. J. Chem.* **1993**, *71*, 1184−1199. (g) Jubert, C.; Nowotny, S.; Kornemann, D.; Antes, I.; Tucker, C. E.; Knochel, P. *J. Org. Chem.* **1992**, *57*, 6384−6386. (h) Nakamura, E.; Kuwajima, I.; Williard, P. G. *Acta Crystallogr.* **1991**, *C47*, 984−985. (i) Joseph-Nathan, P.; Villagomez, J. R.; Rajos-Gardida, M.; Roman, L. U.; Hernandez, J. D. *Phytochemistry* **1989**, *28*, 2397−2401. (j) Lodge, E. P.; Heathcock, C. H. *J. Am. Chem. Soc.* **1987**, *109*, 3353−3361. (k) Haner, R.; Schweizer, W. B.; Seiler, P.; Seebach, D. *Chimia*, **1986**, *40*, 97−98. (l) Heathcock, C. H.; Young, S. D.; Hagen, J. P.; Pirrung, M. C.; White, C. T.; VanDerveer, D. *J. Org. Chem.* **1980**, *45*, 3846−3856. (m) Harlow, R. L.; Simonsen, S. H. *Cryst. Struct. Commun.* **1976**, *5*, 471−476.

(9) Stiles, M.; Winkler, R. R.; Chang, Y.-L.; Traynor, L. *J. Am. Chem. Soc.* **1964**, *86*, 3337−3342.

(10) House, H. O.; Crumrine, D. S.; Teranishi, A. Y.; Olmstead, H. D. *J. Am. Chem. Soc.* **1973**, *95*, 3310−3324.

(11) Zimmerman, H. E.; Traxler, M. D. *J. Am. Chem. Soc.* **1957**, *79*, 1920−1923.

(12) The six-membered structures do not contain any unfavored 1,3-diaxial repulsion, because the C═O plane is included in the ring to make only the π orbitals axial.

(13) (a) Canceill, J.; Basselier, J.-J.; Jacques, J. *Bull. Soc. Chim. Fr.* **1967**, 1024−1030. (b) Auerbach, R. A.; Kingsbury, C. A. *Tetrahedron* **1971**, *27*, 2069−2078. (c) Mulzer, J.; Zippel, M.; Brüntrup, G.; Segner, J.; Finke, J. *Liebigs Ann. Chem.* **1980**, 1108−1134. (d) Heng, K. K.; Simpson, J.; Smith, R. A. J. *J. Org. Chem.* **1981**, *46*, 2932−2934.

(14) Gaudemer, A. In *Stereochemistry, Fundamentals and Methods*; Kagan, H. B., Ed.; Thieme: Stuttgart, 1977; Vol. I, pp 69−71.

(15) Quinkert, G.; Egert, E.; Greisinger, C. In *Aspects of Organic Chemistry: Structure*; VCH: Weinheim, 1996; pp 431−434.

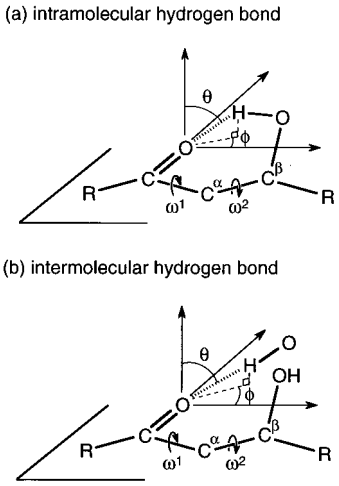

Figure 3. Geometric parameters for aldols. The ω^1 and ω^2 values are defined as the O═C─C(α)─C(β) and C─C(α)─C(β)─O dihedral angles, respectively. The θ and ϕ parameters show hydrogen-bond directionality in a spherical coordinate system.

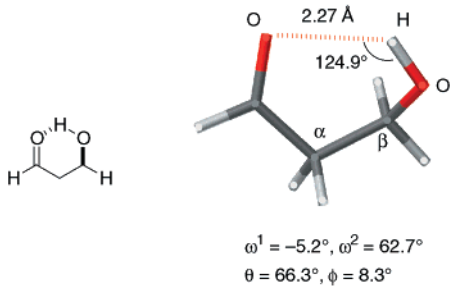

Figure 4. Structure of 3-hydroxypropanal obtained by DFT calculation at the B3LYP/6-311++G(d,p) level. For definitions of ω^1, ω^2, θ, and ϕ, see Figure 3.

Aldols are ketones or aldehydes that possess a hydroxyalkyl group at C(α). Thus, unless otherwise constrained, the energy minima are obtained primarily at O═C─C(α)─C(β) dihedral angles (ω^1) of 0, 120, and −120°, and C(C═O)─C(α)─C(β)─O dihedral angles (ω^2) of 60, 180, and −60°. Figure 3 shows the general geometries of aldols having an intramolecular and intermolecular hydrogen bond. The position of the OH proton is defined by the angles θ and ϕ in the polar coordinates. The *syn*-C═O/OH eclipsed conformation of 3-hydroxypropanal in Figure 2 has $\omega^1 = 0°$ and $\omega^2 = 60°$ and is distinct from the half-chair conformation with $\omega^1 = \omega^2 = 60°$, $\theta = 90°$, and $\phi = 30°$. The presence of an intramolecular hydrogen bond only slightly distorts the eclipsed geometry, as illustrated in Figure 4. A density functional theory (DFT) calculation at the B3LYP/6-311++G(d,p) level led to an optimized geometry at $\omega^1 = -5.2°$, $\omega^2 = 62.7°$, $\theta = 66.3°$, and $\phi = 8.3°$. Because of the electrostatic nature of the OH···O═C interaction with a little charge-transfer contribution (∼20%), the coplanarity ($\theta = 90°$) seen in the half-chair form is not requisite for the cyclic structure. In addition, the ϕ value is close to 0° but not to 30°. The hydrogen bond stabilizes the six-membered cyclic structure by 3.8 kcal/mol, in comparison to the non-hydrogen-bonded *syn*-C═O/OH structure (destabilized by a dipole repulsion), and by 2.6 kcal/mol with respect to the *anti*-C═O/OH conformation. Thus, the calculation suggests that simple aldols in a vacuum inherently favor the eclipsed conformation, where the torsional strain is the major factor controlling the geometry. With skeletally flexible aldols, nine staggered conformers are possible, while two of these conformers having a *syn*-C═O/OH relation ($\omega^1 = 0°$ and $\omega^2 = 60$ or −60°) are stabilized by an intramolecular hydrogen bond. In accord with this view, the Cambridge crystallographic data of certain crystalline, intramolecularly hydrogen-bonded acyclic aldols gave the values of $\omega^1 = -14.4°$, $\omega^2 = 57.9°$ (or −4.4° and 72.6°, respectively), $\theta = 78.1°$, and $\phi = 7.4°$.

In certain cases, an intramolecular hydrogen bond forms at the cost of an increase in torsional strain. Thus, some oligomeric or polymeric aldols having a similar conformation would form via intermolecular hydrogen bonds. Here, the stabilization might be achieved with an ideal in-plane OH···O═C interaction ($\theta = 90°$).

Results and Discussion

We investigated here the structures of typical cycloalkanone-derived aldol systems in which stereochemical and structural determinants are systematically incorporated. The three sets of threo and erythro aldols **1**−**3** were selected, because these are products of standard stereoselective aldol reactions and also are pertinent to the stereochemical argument. Compounds **1** and **2** are constructed from cyclohexanones and aldehydes, the difference being the absence or presence of a trans alkyl substituent at C(3). Setting the dihedral angle ω^1 to ∼0 or 120° simplifies the argument. The aldols **3** are cyclopentanones possessing vicinal, trans substituents at C(2) and C(3). Molecular modeling suggests that, unlike in the cyclohexanone aldols **2**, the ω^1 value is forced to increase to 45 or 75° for the half-chair form and to 60° for the envelope structure (computer modeling). The relative stabilities of aldol conformers are further controlled by various attractive and repulsive interactions. Subtype **a** ($R^\beta = c\text{-}C_6H_{11}$) denotes the aldols produced from cyclohexanecarbaldehyde, while subtype **b** ($R^\beta = C_6H_5$) aldols are derived from benzaldehyde. The difference in the aliphatic and aromatic groups may affect the conformational stability of the aldols.

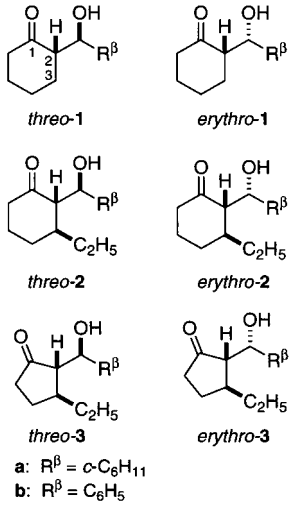

The degree of aggregation was determined by a cryoscopic method, while the nature of the hydrogen bonds was elucidated by IR and NMR. A detailed examination revealed that the unambiguous determination of relative configuration can be made only by X-ray crystallographic analysis or chemical transformation from/to stereoauthentic compounds. The conformations in the crystalline and solution phases were shown to be subtly affected by various intramolecular and intermolecular forces. NMR analysis provided useful information for the structures in solution, but such data should be treated carefully.

Preparation of Standard Aldols. Racemic aldols were used for this investigation. Diastereomeric *threo*- and *erythro*-**1a** were

synthesized stereoselectively by reacting lithium[16] and tetrabutylammonium[17] enolate of cyclohexanone with cyclohexanecarbaldehyde, respectively. A 33:67 mixture of *threo*-**1b** and *erythro*-**1b** was prepared by the reaction of cyclohexanone and benzaldehyde in aqueous sodium hydroxide solution.[18] The C(3)-ethylated compounds, *threo*-**2a** and *threo*-**3a**, were synthesized with a > 99:1 stereoselectivity by Cu(I)-catalyzed 1,4-addition[19] of diethylzinc to 2-cyclohexenone or 2-cyclopentenone, followed by the trapping of the in situ formed ethylzinc enolates with cyclohexanecarbaldehyde. The vicinal carbon−carbon bond formation occurred with perfect trans selectivity. With benzaldehyde, the aldols **2b** and **3b** were produced as 81:19 and 55:45 mixtures of threo and erythro isomers. When boron trifluoride was added in the Zn enolate reaction, *threo*- and *erythro*-**2a** were produced in a 50:50 ratio. All the stereochemically pure aldols were obtained by chromatographic separation followed by recrystallization, if possible. The eleven different aldols thus obtained were subjected to structural elucidation by molecular weight measurement, NMR and IR spectroscopy, and X-ray diffraction.

Molecular Structures in Crystalline State: X-ray Structural Analysis. The configurations of the crystalline aldols **1**−**3** were determined by X-ray analysis. Noncrystalline *threo*-**3b** was derivatized to the crystalline *p*-bromobenzoate whose structure was analyzed by X-ray diffraction. Single crystals of *threo*-**1a**, *erythro*-**1a**, *threo*-**1b**, *erythro*-**1b**, *threo*-**2a**, *erythro*-**2a**, *threo*-**2b**, *erythro*-**2b**, *threo*-**3a**, and *erythro*-**3b** were obtained by recrystallization, while *threo*-**3b** did not crystallize. These crystallographic data are summarized in Table 1. Figure 5 shows the molecular structures with selected interatomic distances, bond angles, dihedral angles, and the position of the hydroxy proton.

The simple cyclohexanone-derived aldols **1** crystallized in the monoclinic system with a $P2_1/a$, $P2_1/c$, or $P2_1/n$ space group. The compounds *threo*-**1a**, *erythro*-**1a**, and *threo*-**1b** contain an intramolecular hydrogen bond forming a six-membered cyclic framework with OH···O═C bond distances of 1.81, 2.48, and 2.15 Å and the O···H−O bond angles of 133.36, 132.0, and 133.03°, respectively. The hydroxy protons are located at the point of $\theta = 55.2-69.7°$ and $\phi = -5.7-10°$, in good agreement with the calculated values for 3-hydroxypropanal (Figure 4). In *erythro*-**1a**, the OH proton interacted not only with the C═O oxygen in the same molecule but also with the C═O of the other enantiomeric aldol, and as a result, the aldol formed a heterochiral dimer. The *erythro*-**1b** crystal has no intramolecular hydrogen bond, but instead, a pair of the enantiomeric aldol molecules form a heterochiral dimer with the $R_2^2(12)$ graph set[20] via an intermolecular OH···O═C interaction. These dimeric aldols have θ and ϕ values of 77.6−89° and 65.2−82.1°, respectively, giving a near-linear OH···O═C bond. The distances between one of the C(3)−H protons and the cyclohexyl methine carbon in *threo*-**1a** and *erythro*-**1a** are 2.22−2.65 and 2.60−2.63 Å, respectively. These values are close to the sum of the van der Waals radii of two hydrogen atoms, 2.4 Å. Notably, replacement of the cyclohexyl with a phenyl group shortened the H···C distances to 2.71 (*threo*-**1b**) and 2.69 (2.76) Å (*erythro*-**1b**), which were 5−8% shorter than the distance of 2.9 Å, indicating the existence of a CH/π interaction between the C(3)−H and the phenyl carbon.[21] As expected, all four of these aldols have an equatorially oriented C(2) substituent, with respect to the chairlike cyclohexanone framework possessing staggered $C(sp^3)-C(sp^3)$ linkages and a small O═C−C(α)−C(β) dihedral angle (ω^1), 2.7−7.6°, close to the standard 0°.

The presence of an ethyl substituent at C(3) totally changes the crystalline structures. The crystals of aldols **2** were monoclinic or tetragonal with a $P2_1/c$, $P2_1/a$, $P4/n$, or Cc space group. None of these crystals had an intramolecular hydrogen bond; rather, the aldol molecules interacted intermolecularly to result in polymeric structures. Among them, *threo*-**2a**, *erythro*-**2a**, and *erythro*-**2b** have an intermolecular hydrogen bond along the direction of the sp^2 lone pair of the carbonyl oxygen ($\theta = 74.7-79.8°$, $\phi = 36.6-45.1°$). The ω^1 dihedral angle ranges from −102.4 to −111.3°, which is to be compared to the standard value of −120°, while the $C(sp^3)-C(sp^3)$ linkages have a normal staggered geometry. The cyclohexanone skeletons are characterized by the trans diaxial substituents at C(2) and C(3), with the dihedral angles ranging from 152 to 168.8°. Such unusual conformations were due to the substantial repulsion of the vicinal large substituents, but the local energetic penalty was compensated for by forming multiple intermolecular hydrogen bonds and by improving the packing efficiency into the unit cell.

The cyclopentanone aldol *threo*-**3a** crystallized in a monoclinic system with a $P2_1/a$ space group, while *erythro*-**3b** crystals had an orthorhombic system with a *Pbca* space group. Both *threo*-**3a** and *erythro*-**3b** form polymeric structures by intermolecular OH···O═C hydrogen bonds. The hydroxy protons are directed toward the oxygen sp^2 lone pair, though not in the C═O plane ($\theta = 54.6-70.4°$, $\phi = 21.4-41.3°$). The cyclopentanone ring of *threo*-**3a** has an envelope conformation with an ω^1 dihedral angle of −56.4°. In *erythro*-**3b**, the cyclopentanone framework takes a half-chair conformation where the ω^1 dihedral angle is −46.7°. These values are significantly different from the −102 to −111° angles for cyclohexanone derivatives **2**. Furthermore, the C−C(2)−C(3)−C dihedral angles involving the C(2) and C(3) substituents, 86.6 and 89.6°, respectively, are much smaller than the values of the trans disubstituted cyclohexanones **2**, 152−169°. In *erythro*-**3b**, a CH/π attraction[21] is present between one of the C(3)−ethyl methylene protons (unlike C(3)−H in *threo*- and *erythro*-**1b**) and the phenyl carbon, as judged by the short H···C distance, 2.69 Å.

Such unique crystalline structures would already recommend the careful use of the Stiles−House structural analysis in solution.

Figure 6 illustrates the statistic lone pair directionality in the OH···O═C interaction in aldols. The data were collected from the present study and the Cambridge Structural Database.[22] The result indicates that the position of the hydroxy proton is highly flexible, depending on the structures. Owing to the skeletal restriction, intramolecularly hydrogen-bonded monomers gave small ϕ values (∼0°), whereas the cyclic dimers gave values larger than 60°. Such skeletal constraints were relieved in the polymeric aldols, which formed intermolecular hydrogen bonds largely along the direction of the C═O sp^2 lone pairs. Such hydrogen bonds are enthalpically more favored. In fact, 21

(16) Yamago, S.; Machii, D.; Nakamura, E. *J. Org. Chem.* **1991**, *56*, 2098−2106.

(17) Noyori, R.; Yokoyama, K.; Sakata, J.; Kuwajima, I.; Nakamura, E.; Shimizu, M. *J. Am. Chem. Soc.* **1977**, *99*, 1265−1267.

(18) Billimoria, J. D. *J. Chem. Soc.* **1955**, 1126−1129.

(19) Kitamura, M.; Miki, T.; Nakano, K.; Noyori, R. *Tetrahedron Lett.* **1996**, *37*, 5141−5144. Kitamura, M.; Miki, T.; Nakano, K.; Noyori, R. *Bull. Chem. Soc. Jpn.* **2000**, *73*, 999−1014.

(20) Bernstein, J.; Davis, R.; Shimoni, L.; Chang, N.-L. *Angew. Chem., Int. Ed. Engl.* **1995**, *34*, 1555−1573. Etter, M. C. *Acc. Chem. Res.* **1990**, *23*, 120−126. Etter, M. C.; MacDonald, J. C.; Bernstein, J. *Acta Crystallogr.* **1990**, *B46*, 256−262. Etter, M. C. *J. Phys. Chem.* **1991**, *95*, 4601−4610.

(21) Nishio, M.; Hirota, M.; Umezawa, Y. *The CH/π Interaction*; Wiley-VCH: New York, 1998; p 66.

(22) Allen, F. H.; Bellard, S.; Brice, M. D.; Cartwright, B. A.; Doubleday, A.; Higgs, H.; Hummelink, T.; Hummelink-Peters, B. G.; Kennard, O.; Motherwell, W. D. S.; Rodgers, J. R.; Watson, D. G. *Acta Crystallogr.* **1979**, *B35*, 2331−2339.

Table 1. Crystallographic Data for **1**, **2**, and **3**[a]

		Compunds **1**		
compound	*threo*-**1a**	*erythro*-**1a**	*threo*-**1b**	*erythro*-**1b**
mol formula	$C_{13}H_{22}O_2$	$C_{13}H_{22}O_2$	$C_{13}H_{16}O_2$	$C_{13}H_{16}O_2$
mol wt	210.31	210.31	204.27	204.27
cryst color, habit	colorless, prismatic	colorless, prismatic	colorless, prismatic	colorless, prismatic
cryst size/mm^3	0.20 × 0.10 × 0.20	0.20 × 0.20 × 0.20	0.20 × 0.20 × 0.50	0.05 × 0.10 × 0.50
cryst syst	monoclinic	monoclinic	monoclinic	monoclinic
lattice type	primitive	primitive	primitive	primitive
space group	$P2_1/a$	$P2_1/c$	$P2_1/n$	$P2_1/a$
a/Å	10.5975(5)	11.465(2)	10.252(3)	15.577(4)
b/Å	10.1387(7)	10.190(1)	11.273(3)	5.714(5)
c/Å	11.5644(5)	11.667(1)	10.421(2)	26.195(3)
α/deg	90	90	90	90
β/deg	100.719(3)	114.924(10)	112.67(2)	106.31(1)
γ/deg	90	90	90	90
vol/Å^3	1220.8(1)	1236.1(3)	1111.3(5)	2237(2)
Z	4	4	4	8
ρ_{calcd}/g cm^{-3}	1.140	1.130	1.215	1.213
total reflections	2054	1606	1861	3884
unique reflections	1940 (R_{int} = 0.022)	1523 (R_{int} = 0.041)	1755 (R_{int} = 0.043)	3731 (R_{int} = 0.105)
corrections	Lorentz polarization	Lorentz polarization absorption (trans. factors: 0.7677−1.0000)	Lorentz polarization secondary extinction (coefficient: 2.05553 × 10^{-5})	Lorentz polarization absorption (trans. factors: 0.6721−1.0000) secondary extinction (coefficient: 3.23304 × 10^{-6})
structure solution	direct methods[b]	direct methods[b]	direct methods[c]	direct methods[c]
no. of observations ($I > 3.00\sigma(I)$)	1276	1337	1058	1709
R	0.070	0.085	0.058	0.055
R_w	0.074	0.107	0.044	0.039
		Compounds **2**		
compound	*threo*-**2a**	*erythro*-**2a**	*threo*-**2b**	*erythro*-**2b**
mol formula	$C_{15}H_{26}O_2$	$C_{15}H_{26}O_2$	$C_{15}H_{20}O_2$	$C_{15}H_{20}O_2$
mol wt	238.37	238.37	232.32	232.32
cryst color, habit	colorless, prismatic	colorless, prismatic	colorless, prismatic	colorless, prismatic
cryst size/mm^3	0.20 × 0.30 × 0.40	0.10 × 0.20 × 0.50	0.50 × 0.50 × 0.30	0.50 × 0.10 × 0.10
cryst syst	monoclinic	monoclinic	tetragonal	monoclinic
lattice type	primitive	primitive	primitive	C-centered
space group	$P2_1/c$	$P2_1/a$	$P4/n$	Cc
a/Å	9.456(2)	9.654(1)	18.217(3)	22.200(7)
b/Å	5.989(1)	13.835(2)	18.217(3)	11.977(4)
c/Å	25.338(1)	10.6001(8)	8.387(3)	10.360(7)
α/deg	90	90	90	90
β/deg	100.40(1)	98.179(8)	90	102.61(4)
γ/deg	90	90	90	90
vol/Å^3	1411.4(5)	1401.3(2)	2782.3(8)	2688(1)
Z	4	4	8	8
ρ_{calcd}/g cm^{-3}	1.122	1.130	1.109	1.148
total reflections	2498	2330	2404	1844
unique reflections	2341 (R_{int} = 0.066)	2187 (R_{int} = 0.027)		1788 (R_{int} = 0.067)
corrections	Lorentz polarization absorption (trans. factors: 0.6915−1.0000) decay (−14.54% decline) secondary extinction (coefficient: 2.64278 × 10^{-6})	Lorentz polarization	Lorentz polarization secondary extinction (coefficient: 4.06736 × 10^{-6})	Lorentz polarization absorption (trans. factors: 0.4504−1.0000) secondary extinction (coefficient: 1.73621 × 10^{-6})
structure solution	direct methods[d]	direct methods[b]	direct methods[d]	direct methods[c]
no. of observations ($I > 3.00\sigma(I)$)	1734	1120	1609	1179
R	0.078	0.051	0.082	0.070
R_w	0.089	0.046	0.077	0.053
		Compounds **3**		
compound	*threo*-**3a**	*erythro*-**3b**		*p*-bromobenzoate of *threo*-**3b**
mol formula	$C_{14}H_{24}O_2$	$C_{14}H_{18}O_2$		$C_{21}H_{21}O_3Br$
mol wt	224.34	218.29		401.30
cryst color, habit	colorless, prismatic	colorless, prismatic		colorless, prismatic
cryst size/mm^3	0.20 × 0.20 × 0.30	0.50 × 0.30 × 0.10		0.30 × 0.30 × 0.30
cryst syst	monoclinic	orthorhombic		monoclinic
lattice type	primitive	primitive		primitive
space group	$P2_1/a$	$Pbca$		$P2_1/n$

Table 1. (Continued)

		Compounds **3** continued	
a/Å	9.249(6)	23.425(4)	10.083(2)
b/Å	14.702(7)	14.245(3)	14.058(1)
c/Å	10.628(6)	7.318(2)	13.804(2)
α/deg	90	90	90
β/deg	110.08(4)	90	98.99(1)
γ/deg	90	90	90
vol/Å^3	1357(1)	2442(1)	1932.7(4)
Z	4	8	4
ρ_{calcd}/g cm^{-3}	1.098	1.187	1.379
total reflections	2261	2126	3217
unique reflections	2117 ($R_{int} = 0.079$)		3028 ($R_{int} = 0.224$)
corrections	Lorentz polarization secondary extinction (coefficient: 1.58036×10^{-5})	Lorentz polarization secondary extinction (coefficient: 9.16900×10^{-6})	Lorentz polarization absorption (trans. factors: 0.4496−1.0000) secondary extinction (coefficient: 2.05595×10^{-7})
structure solution	direct methods[e]	direct methods[c]	direct methods[d]
no. of observations ($I > 3.00\sigma(I)$)	1158	1300	2292
R	0.065	0.068	0.125
R_w	0.074	0.066	0.134

[a] Function minimized by $\sum\omega(|F_o| - |F_c|)^2$. [b] SIR92: Altomare, A.; Burla, M. C.; Camalli, M.; Cascarano, M.; Giacovazzo, C.; Guagliardi, A.; Polidori, G. *J. Appl. Crystallogr.* **1994**, 435. [c] SAPI91: Fan, H.-F. *Structure Analysis Program with Intelligent Control*; Rigaku Corporation: Tokyo, Japan, 1991. [d] SIR88: Burla, M. C.; Camalli, M.; Cascarano, G.; Giacovazzo, C.; Guagliardi, A.; Polidori, G.; Spagna, R.; Viterbo, D. *J. Appl. Crystallogr.* **1989**, 389. [e] SAPI90: Fan, H.-F. *Structure Analysis Program with Intelligent Control*; Rigaku Corporation: Tokyo, Japan, 1990.

compounds among the total of 36 crystalline aldols were polymeric, indicating that intermolecular hydrogen bonds facilitate crystal lattice formation.

Molecular Weight Determination. The conformational analysis in solution (Figure 1) assumes the monomeric structures for aldols. The aggregation states of the aldols **1**−**3** in hydrocarbons were determined by a cryoscopic molecular weight measurement using a 100−500 mM benzene solution or a ∼10 mM cyclohexane solution. The number-average molecular weight (MW_{obs}) and the aggregation state (MW_{obs}/MW_{calcd}) were calculated on the basis of the molar depression values of 5.16[23] (benzene) and 22.3 (cyclohexane) and the monomeric molecular weights of 210.32 (**1a**), 204.27 (**1b**), 238.37 (**2a**), 232.32 (**2b**), 224.34 (**3a**), and 218.29 (**3b**). The results are listed in Table 2. In all cases, the MW_{obs}/MW_{calcd} ratio ranged between 1 and 2, indicating that the aldols exist as an equilibrium mixture of the monomer and some aggregates. In a 10−13 mM cyclohexane solution at ∼6 °C, *threo*-**1a**, *erythro*-**1a**, *threo*-**1b**, *erythro*-**1b**, *threo*-**2a**, *erythro*-**2a**, *threo*-**3a**, and *threo*-**3b** gave an MW_{obs}/MW_{calcd} value of 0.95−1.25, suggesting the preference for the monomeric form. With *threo*-**2b** and *erythro*-**2b** under similar conditions, however, the values were increased to 1.47−1.62 and 1.72−1.96, respectively. Assuming a monomer−dimer equilibrium, 63−77% of *threo*-**2b** and 84−98% of *erythro*-**2b** exist in the dimeric form, although the participation of higher aggregates is also conceivable. The high crystallinity of *erythro*-**3b** did not allow a molecular weight measurement. In more polar benzene, the MW_{obs}/MW_{calcd} value of all aldols never exceeded 1.13, even in a solution with a concentration that was 10 times higher. However, when the concentration was increased from 100 mM to 300 or 500 mM, the aldols behaved similarly to those in a 10 mM cyclohexane solution. Thus, the aggregation states of *threo*- and *erythro*-**1a**, *threo*- and *erythro*-**1b**, and *threo*-**2a** were in the range 1.05−1.24, while the values of *erythro*-**2a**, *threo*-**2b**, and *erythro*-**2b** were higher, from 1.44 to 1.66. Thus, 61−80% of these aldols exist as dimers in solutions with concentrations greater than 300 mM.

(23) Kitamura, M.; Okada, S.; Suga, S.; Noyori, R. *J. Am. Chem. Soc.* **1989**, *111*, 4028−4036.

Infrared Spectroscopy. To suitably evaluate the solution structures of aldols **1**−**3**, the patterns of hydrogen bonds must be clarified. To detect the presence and define the nature of these aldols, whether hydrogen-bonded intramolecularly or intermolecularly, their IR spectra were taken by changing the concentration from 100 to 500 mM in benzene. Table 3 shows the observed stretching vibration absorption bands of the hydroxy and carbonyl groups. Although a similar aggregation state is accessible in cyclohexane at a concentration of lower than ∼15 mM, reliable spectra with a reasonable signal-to-noise ratio could not be obtained.

Because the frequency is proportional to the square root of the reduced mass, O−H bands are more sensitive to hydrogen bonding than C═O bands. At a concentration of 100 mM in benzene, *threo*-**1a**, *erythro*-**1a**, *threo*-**1b**, *erythro*-**1b**, *threo*-**2a**, *threo*-**3a**, and *threo*-**3b** exhibited broad O−H bands at 3477−3577 cm^{-1}, and in the range 100−500 mM, virtually no band shifts were observed. The broad shape of signals with no concentration effect indicates the presence of intramolecular hydrogen bonds in these aldols. On the other hand, one sharp and one broad band were observed in a ∼3:1 ratio at 3604 and 3475 cm^{-1} for *erythro*-**2a**, and at 3576 and 3483 cm^{-1} for *erythro*-**2b** in 100 mM benzene solutions. The ratio of the two bands was changed to ∼1:1 as the concentration was increased to 500 mM. A 100 mM benzene solution of *erythro*-**3b** also exhibited a sharp band at 3581 cm^{-1} and a broad one at 3491 cm^{-1}; a good spectrum could not be obtained at concentrations greater than 300 mM, owing to the solubility problem. The sharp and broad bands are assignable to the stretching vibrations of a free hydroxy and intermolecularly hydrogen-bonded hydroxy group, respectively. A 100 mM solution of *threo*-**2b** exhibited one sharp and two broad bands in a ∼2:2:1 ratio at 3567, 3512, and 3424 cm^{-1}, respectively. In a 500 mM solution, the intensity of the 3567 cm^{-1} band was halved, while the strength of the 3424 cm^{-1} band was doubled, with the 3512 cm^{-1} band remaining unchanged. These bands can be assigned to free, intramolecularly hydrogen-bonded and intermolecularly hydrogen-bonded hydroxy groups, respectively. These IR observations are consistent with the cryoscopic experiments. The compounds

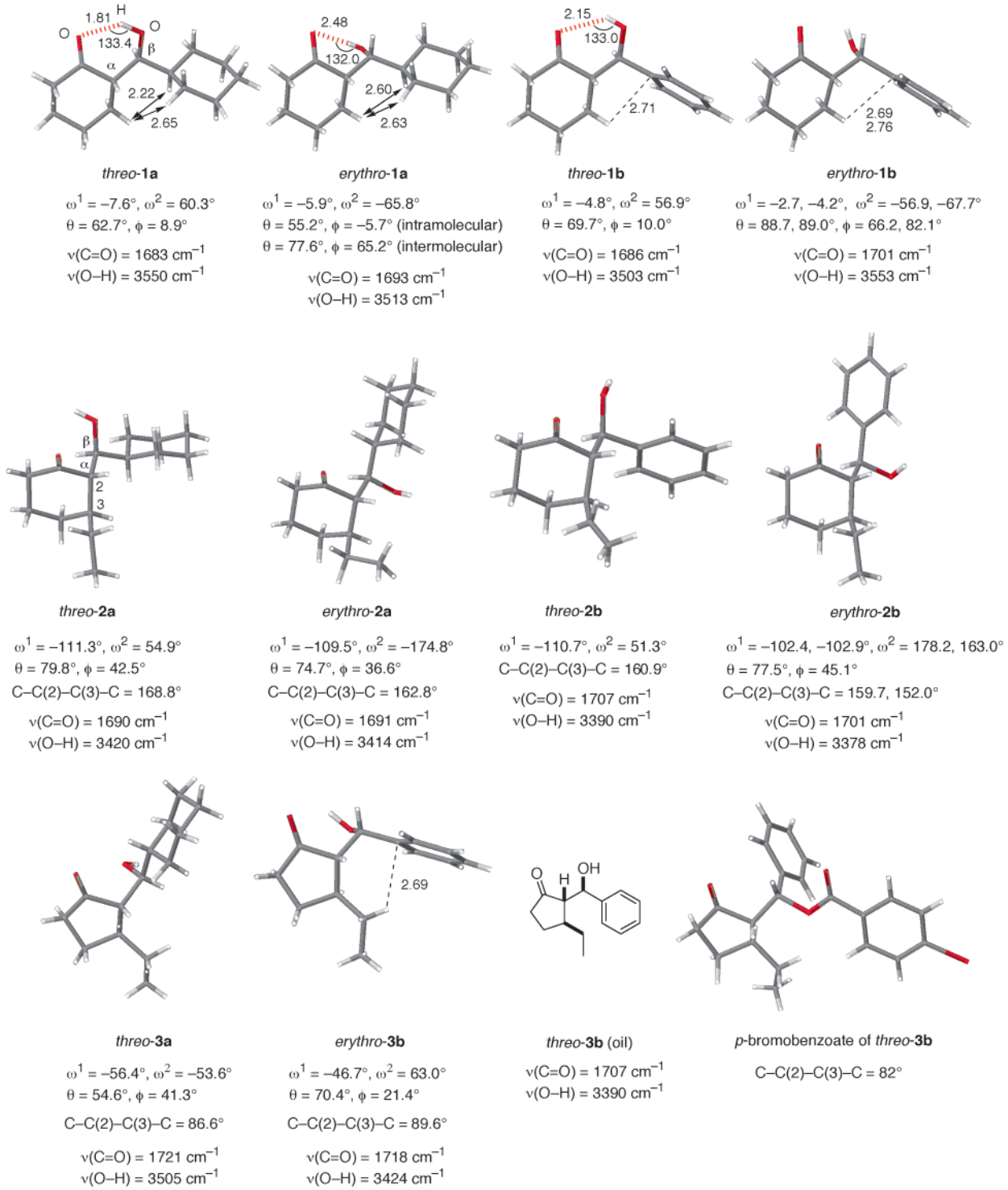

Figure 5. Molecular structures of the aldols **1**−**3** in the crystalline state. The interatomic distances are in angstroms, and the angles are in degrees. The dotted and broken lines indicate hydrogen bonds and CH/π interactions, respectively. For definitions of ω^1, ω^2, θ, and ϕ, see Figure 3. The IR data were taken by a KBr method.

forming intermolecular hydrogen bonds tended to show higher aggregation states.

NMR Spectroscopy. NMR spectra provide various information about the aldol structures in solution. ^{1}H and ^{13}C NMR experiments were conducted in 10 and 2 mM cyclohexane-d_{12} solutions at 23 °C to investigate the presence of hydrogen bonds and to obtain conformational information on the aldol molecules in solution. The results are shown in Table 4.

The ^{1}H and ^{13}C chemical shifts of C(α)H and C(β)H were insensitive to concentration. The hydroxy protons involved in intermolecular hydrogen bonds, however, tended to give signals at a higher magnetic field as concentrations were lowered, because the degree of the magnetic shielding effect was increased as the hydrogen bond became weak.

The ^{1}H chemical shifts of OH were little affected by the concentration of *threo*-**1a**, *erythro*-**1a**, *threo*-**1b**, *erythro*-**1b**, *threo*-**2a**, *threo*-**3a**, or *threo*-**3b**. This phenomenon was attributed to the absence of an intermolecular hydrogen bond and probably to the formation of an intramolecular hydrogen bond. In the cases of *erythro*-**2a**, *threo*-**2b**, and *erythro*-**2b**, the OH signal

Table 2. Molecular Weights and Aggregation States of Aldols **1**−**3**

compound	solvent	conc, mM	MW_{obs}	MW_{obs}/MW_{calcd}[a]	aggregation state in crystal
threo-**1a**	benzene	300	221−229	1.05−1.09	monomer
	benzene	200	204−229	0.97−1.09	
	benzene	100	192−201	0.91−0.96	
	cyclohexane	13	253	1.20	
erythro-**1a**	benzene	300	223−226	1.06−1.07	dimer
	benzene	200	228−230	1.08−1.09	
	benzene	100	222−226	1.05−1.07	
	cyclohexane	13	245−261	1.17−1.25	
threo-**1b**	benzene	300	217−230	1.06−1.13	monomer
	benzene	200	230−242	1.13−1.19	
	benzene	100	210−226	1.03−1.11	
	cyclohexane	13	223−230	1.09−1.12	
erythro-**1b**	benzene	300	241−243	1.18−1.19	dimer
	benzene	200	226−228	1.11−1.12	
	benzene	100	190−210	0.93−1.03	
	cyclohexane	13	193−215	0.95−1.05	
threo-**2a**	benzene	500	291−296	1.22−1.24	polymer
	benzene	300	274−282	1.15−1.18	
	benzene	100	247−270	1.03−1.13	
	cyclohexane	13	245−259	1.03−1.09	
erythro-**2a**	benzene	500	344−352	1.44−1.48	polymer
	benzene	300	302−308	1.26−1.29	
	benzene	100	246−255	1.03−1.07	
	cyclohexane	13	271−298	1.14−1.25	
threo-**2b**	benzene	500	379−385	1.63−1.66	tetramer
	benzene	300	332−340	1.43−1.46	
	benzene	100	237−241	1.02−1.04	
	cyclohexane	11	341−377	1.47−1.62	
erythro-**2b**	benzene	500	340−345	1.46−1.48	polymer
	benzene	300	303−310	1.30−1.33	
	benzene	100	245−250	1.05−1.07	
	cyclohexane	10	399−456	1.72−1.96	
threo-**3a**	cyclohexane	13	232−246	1.04−1.10	polymer
threo-**3b**	cyclohexane	13	239−261	1.10−1.20	−
erythro-**3b**	cyclohexane	5−13[b]	−	−	polymer

[a] MW_{calcd}: **1a** (210.32), **1b** (204.27), **2a** (238.37), **2b** (232.32), **3a** (224.34), **3b** (218.29). [b] Crystallization occurred during measurement.

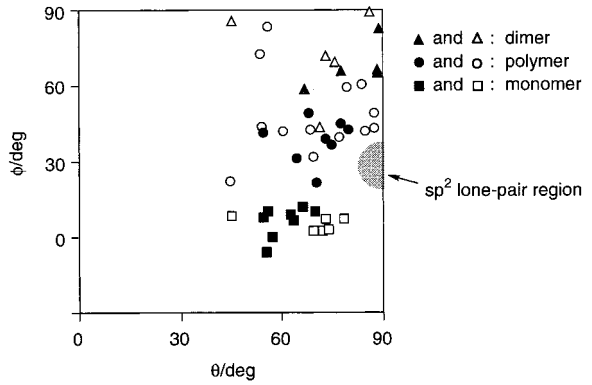

Figure 6. Plots of the lone pair directionality in OH···O═C bonds. The filled symbols refer to the results obtained in our laboratories (unpublished data included). The open symbols refer to the values taken from the Cambridge Structural Database.

shifted from δ 1.65 to 1.60, from δ 3.37 to 3.31, and from δ 2.87 to 2.78, respectively, upon decreasing the concentration from 10 to 2 mM. The higher-field shift by 0.05−0.09 ppm revealed the presence of an intermolecular hydrogen bond. This interpretation is in full accord with the cryoscopic and IR analyses. The presence of an intermolecular hydrogen bond in *erythro*-**3b** was suggested by the IR and molecular weight measurement but remained unclear. However, the presence of such a bond was verified by NMR analysis, which showed the OH signal at δ 2.77 in a 10 mM solution and δ 2.69 in a 2 mM solution, both at 50 °C.

Validity of the Stiles−House Rule. Thanks to their high sensitivity to conformations, NMR coupling constants have frequently been used for the configurational assignment of aldols (Stiles−House rule). For such an assignment, the aldol must have a monomeric, intramolecularly hydrogen-bonded, six-membered structure for the conformational arguments of Figure 1. Judging from the cryoscopic, IR, and NMR study, the four aldols of series **1**, *threo*-**2a**, *threo*-**3a**, and *threo*-**3b** are suitable for the NMR analysis, because they satisfy the prerequisite in a hydrocarbon solution. If applied rigorously, only series **1** fulfills Stiles' original criteria,[9] where both threo and erythro diastereomers have equally monomeric, hydrogen-bonded structures in solution. Great care must be taken for the other aldols with intermolecular hydrogen bonds. In the case of **2a**, **3a**, and **3b**, only one of these diastereomers satisfies the conditions for analysis.

The $J_{\alpha,\beta}$ values of the simple cyclohexanone-derived aldols **1** are fully consistent with the Stiles−House empirical rule that a threo isomer exhibits the vicinal coupling constant of 6−9 Hz, and an erythro isomer 2−4 Hz.[10] In fact, *threo*-**1a**, *erythro*-**1a**, *threo*-**1b**, and *erythro*-**1b** gave the $J_{\alpha,\beta}$ values 7.3, 2.7, 8.8, and 2.4 Hz, respectively. These aldols are thought to have the T_{ap} or E_{-sc} conformations, shown in Figure 1 (also Figure 3a) with an equatorial C(β) substituent. The crystalline state structures of Figure 5 also fit with this view, with the exception of *erythro*-**1b**, which forms intermolecular hydrogen bonds (Figure 3b).

The Stiles−House rule does not apply for aldols **2** having an ethyl substituent at C(3). Instead, the forcing application leads to an erroneous, opposite assignment for *threo*-**2a** and *erythro*-**2a**. Thus, the threo isomer is monomeric and does form an intramolecular hydrogen bond, but the observed $J_{\alpha,\beta}$ value of

Table 3. Infrared Stretching Absorption Bands of Hydroxy and Carbonyl Groups of Aldols **1**−**3** in Benzene[a]

		frequency, cm^{-1}	
compound	conc, mM	O−H	C=O
threo-**1a**	500	3553	1697
	300	3553	1697
	100	3553	1697
erythro-**1a**	500	3574	1701
	300	3575	1701
	100	3577	1701
threo-**1b**	500	3573	1698
	300	3573	1698
	100	3573	1698
erythro-**1b**	500	3573	1701
	300	3573	1701
	100	3573	1701
threo-**2a**	500	3541	1698
	300	3542	1698
	100	3542	1698
erythro-**2a**	500	3604 (s), 3475 (br) (∼1:1)	1705
	300	3604 (s), 3475 (br) (∼2:1)	1705
	100	3604 (s), 3475 (br) (∼3:1)	1706
threo-**2b**	500	3567 (s), 3506 (br), 3424 (br) (∼1:2:2)	1702
	300	3567 (s), 3512 (br), 3424 (br) (∼3:4:3)	1702
	100	3567 (s), 3512 (br), 3424 (br) (∼2:2:1)	1701
erythro-**2b**	500	3571 (s), 3464 (br) (∼1:1)	1702
	300	3575 (s), 3474 (br) (∼2:1)	1702
	100	3576 (s), 3483 (br) (∼3:1)	1703
threo-**3a**	500	3492	1726
	300	3492	1726
	100	3492	1726
threo-**3b**	500	3477	1722
	300	3477	1722
	100	3477	1722
erythro-**3b**	300[b]	–	–
	100	3581 (s), 3491 (br) (∼2:1)	1741

[a] Measured at 23 °C using an optical path length of 0.025 mm. [b] Unmeasurable because of the low solubility.

2.3 Hz nevertheless disagrees with the expected 6−9 Hz value. Furthermore, the erythro isomer equilibrating with the dimer gave a value of 7.3 Hz, rather than the expected 2−4 Hz. Thus, the relative magnitudes were reversed. In a similar manner, *threo*-**2b** and *erythro*-**2b**, which exist as an equilibrium mixture of the monomer and aggregates, gave $J_{\alpha,\beta}$ values 3.9 and 4.4 Hz, values totally different from the 6−9 and 2−4 Hz values predicted from the empirical rule, respectively.

The vicinal coupling constants of cyclopentanone aldols *threo*- and *erythro*-**3b** (7.8 and 3.0 Hz) seem consistent with the empirical rule. However, no intramolecular hydrogen bond is observed in the erythro isomer.

Origin of Conformational Preference. The conformational issue is twofold, involving both the cycloalkanone geometry and the aldol structure, and these two are interrelated. The structures of **1**−**3** in solution, inferred from NMR, do not always follow those in crystals, which are determined by the total balance of a variety of weak forces working in an intra- or intermolecular way. Many of the aldols are flexible and are in an equilibrium of various conformers in solution. Figure 7 depicts six staggered conformations possible for each threo and erythro isomer of cyclohexanone aldols **1** and **2**. The prefixes eq and ax refer to the diequatorial and diaxial orientations, regarding the C(2) and C(3) substituents in the ring. As noted earlier, T and E represent threo and erythro relative configurations, while ap, +sc, and −sc express antiperiplanar, (+)-synclinal, and (−)-synclinal staggered conformations in terms of H^{α} and H^{β}, respectively. Among various conformers, only eq-T_{ap}, eq-T_{+sc}, eq-E_{+sc}, and eq-E_{-sc} involve an intramolecular hydrogen bond. The reported J values of the rigidly fixed steroidal aldols[24] suggest that the vicinal coupling in T_{ap} and E_{ap} with an $H^{\alpha}-C-C-H^{\beta}$ dihedral angle of 180° is 10 Hz, and the values of other synclinal conformers with the dihedral angle of 60° are 2 Hz. Table 5 summarizes the distribution of conformers of the aldols inferred from the NMR coupling constants.

The substituents of cyclohexanone rings tend to take an equatorial orientation, but the geometry of **1** and **2** is influenced by the aldol moiety that forms intramolecular or intermolecular hydrogen bonds. The conformation of the six-membered ring is largely affected by the substituents (Figure 8) and various intermolecular interactions. Notably, *threo*-**2a**, *threo*-**2b**, and *erythro*-**2b** gave a large coupling constant between C(2)H and C(3)H (8−9.3 Hz), indicating the chairlike cyclohexanone structure with two equatorial substituents (Figure 8). In contrast, in all of the crystals of **2**, the cyclohexanone ring has a diaxial conformer (Figure 5). The smaller $J_{2,3}$ value (4.9−5.4 Hz) for *erythro*-**2a** suggests the contribution of such a diaxial conforma-

Table 4. Selected ^1H and ^{13}C NMR Data for **1**, **2**, and **3** in Cyclohexane-d_{12} at 23 °C

		^1H NMR					^{13}C NMR		
		δ, ppm			coupling constant, Hz		δ, ppm		
compound	conc, mM	O*H*	C(*β*)*H*	C(α)*H*	$J_{\alpha,\beta}$	$J_{2,3}$	*C*(C=O)	*C*(α)	*C*(*β*)
threo-**1a**	10	3.04	3.40	2.36	7.3	–	213.0	53.7	75.8
	2	3.03	3.39	2.36	7.3	–	213.0	53.7	75.8
erythro-**1a**	10	2.43	3.69	2.32	2.7	–	212.2	53.0	73.3
	2	2.42	3.69	2.32	2.7	–	212.2	53.0	73.3
threo-**1b**	10	3.69	4.63	2.38	8.8	–	212.6	58.9	75.3
	2	3.68	4.63	2.38	8.8	–	212.6	58.9	75.3
erythro-**1b**	10	2.87	5.30	2.45	2.4	–	212.2	58.3	70.9
	2	2.86	5.30	2.45	2.4	–	212.2	58.3	70.9
threo-**2a**	10	2.36	3.15	2.29	2.3	9.3	213.5	56.2	74.6
	2	2.35	3.15	2.29	2.3	9.3	213.5	56.2	74.6
erythro-**2a**	10	1.65	3.72	2.33	7.3	5.4	210.3	59.4	75.0
	2	1.60	3.72	2.32	7.3	4.9	210.2	59.4	75.0
threo-**2b**	10	3.37	4.81	2.57	3.9	9.3	212.2	61.7	72.0
	2	3.31	4.79	2.58	3.9	9.3	212.2	61.7	72.0
erythro-**2b**	10	2.87	5.14	2.53	4.4	8.1	211.9	61.6	72.8
	2	2.78	5.14	2.53	4.4	8.0	211.9	61.6	72.8
threo-**3a**	10	2.56	3.24	1.84	5.4	*a*	219.2	56.4	76.3
	2	2.55	3.25	1.84	5.4	*a*	*b*	56.4	76.4
threo-**3b**	10	3.94	4.62	1.95	7.8	*a*	220.1	60.8	76.0
	2	3.93	4.62	1.95	7.8	*a*	220.0	60.8	76.0
erythro-**3b**[c]	10	2.77	5.11	2.06	3.0	*a*	218.8	61.0	73.3
	2	2.69	5.11	2.06	3.0	*a*	*b*	*b*	*b*

[a] Unassignable because of signal overlapping. [b] Data could not be obtained with an acceptable signal-to-noise ratio. [c] At 50 °C.

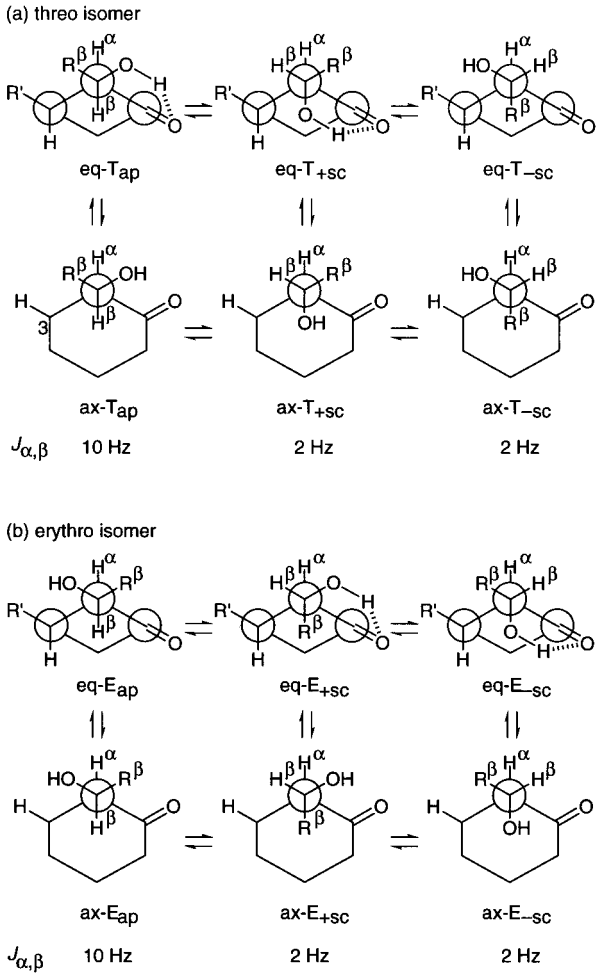

Figure 7. Staggered conformations of (a) threo and (b) erythro cyclohexanone aldols **1** and **2** ($R^{\beta} = C_6H_5$ or *c*-C_6H_{11}; R′ = H or C_2H_5). In the diaxial conformers, R′ is behind C(3) of cyclohexanone.

Table 5. Distribution of Conformers of Aldols **1**−**3** in Cyclohexane-d_{12}[a]

	conformers						cryst
	eq-T_{ap}	eq-T_{+sc}	eq-T_{-sc}	ax-T_{ap}	ax-T_{+sc}	ax-T_{-sc}	struct
threo-**1a**	65	35	0	0	0	0	eq-T_{ap}
threo-**1b**	85	15	0	0	0	0	eq-T_{ap}
threo-**2a**	5	95	0	0	0	0	ax-T_{ap}
threo-**2b**	85	15	0	0	0	0	ax-T_{ap}
threo-**3a**	50	50	0	0	0	0	eq-T_{+sc}
threo-**3b**	75	25	0	0	0	0	−

	eq-E_{ap}	eq-E_{+sc}	eq-E_{-sc}	ax-E_{ap}	ax-E_{+sc}	ax-E_{-sc}	cryst struct
erythro-**1a**	0	0	∼100	0	0	0	eq-E_{-sc}
erythro-**1b**	0	0	∼100	0	0	0	eq-E_{-sc}
erythro-**2a**	30	(35)[b]	(35)[b]	35	0	0	ax-E_{ap}
erythro-**2b**	25	(70)[b]	(70)[b]	5	0	0	ax-E_{ap}
erythro-**3b**	(10)[c]	(90)[b]	(90)[b]	(10)[c]	0	0	eq-E_{-sc}

[a] Distributions in percentage inferred from coupling constant. [b] Conformer could not be specified by NMR. Sum of eq-E_{+sc} and eq-E_{-sc}. [c] Preference could not be specified. Sum of eq-E_{ap} and ax-E_{ap}.

tion or a deformed chair structure in solution as well. Major factors which affect the aldol structures will be discussed by taking typical examples.

A. Hydrogen Bonds. 2-Substituted cyclohexanones take a chair conformer possessing an equatorially oriented substituent.

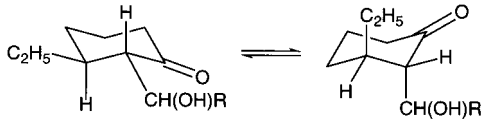

Figure 8. Diequatorial (eq) and diaxial (ax) conformations of 2,3-disubstituted cyclohexanones.

This geometry is further stabilized by the presence of the aldol moiety forming an intramolecular OH···O═C hydrogen bond. The monomeric *threo*-**1a** existed in an equilibrium between eq-T_{ap} and eq-T_{+sc} in favor of the former, as judged from the $J_{\alpha,\beta}$ of 7.3 Hz. The phenyl substituted *threo*-**1b** also showed the same trend. The major eq-T_{ap} conformers were seen in crystalline structures (Figure 5).

Compounds *erythro*-**1a** and *erythro*-**1b** are also monomeric and intramolecularly hydrogen-bonded. The small $J_{\alpha,\beta}$ values < 3 Hz suggest the preference of eq-E_{+sc} or eq-E_{-sc}. These aldols would exist largely (∼100%) as eq-E_{-sc} in solution, just as in the crystalline state (Figure 5). In fact, *erythro*-**1a** in a 10 mM cyclohexane-d_{12} solution at 25 °C showed a 2.5% NOE between C(α)H and the cyclohexyl methine proton. Similarly, with *erythro*-**1b**, a 1.2% NOE was seen between C(α)H and the ortho protons in the phenyl substituent. The ^{1}H NMR spectra of these aldols taken as a 300 mM toluene-d_8 solution gave a single set of signals with the same line shapes at both 25 °C and a low temperature (−78 °C for *erythro*-**1a** and −20 °C for *erythro*-**1b**), although the chemical shifts varied considerably. The stability of the eq-E_{-sc} would be partially ascribed to the σC(α)−H/σ*C(β)−OH orbital interaction.

The effects caused by intermolecular hydrogen bonds are unpredictable. Notably, however, *erythro*-**2a** showed $J_{2,3}$ values of 5.4 and 4.9 Hz in 10 and 2 mM cyclohexane solutions, respectively. The higher concentration increased the number of intermolecular hydrogen bonds, which in turn enhanced the contribution of the ax-E_{ap} conformer. A similar trend was seen in *erythro*-**2b**.

B. Steric Effects of the C(3) Substituents. The C(3)-ethylated aldol, *threo*-**2a**, is a monomer with an intramolecular hydrogen bond in cyclohexane. Unlike *threo*-**1a** favoring eq-T_{ap} ($J_{\alpha,\beta}$ = 7.3 Hz), it existed mostly (95%) as eq-T_{+sc} ($J_{\alpha,\beta}$ = 2.3 Hz), owing to the gauche interaction between the C(2) and C(3) substituents. This aldol still prefers a diequatorial conformer in solution, but the repulsive interaction becomes prominent in the crystalline state, to result in the diaxial conformer ax-T_{ap}. In the erythro isomers, the gauche interaction destabilizes both eq-E_{+sc} and eq-E_{-sc}. Consequently, the intramolecular hydrogen bond is removed to result in eq-E_{ap} and ax-E_{ap}, which in turn are stabilized by intermolecular hydrogen bonds. Such an effect is also seen in *erythro*-**2a** with $J_{\alpha,\beta}$ = 7.3 and $J_{2,3}$ = 5 Hz.

C. CH/π Attraction. The cyclohexyl (**a** series) and phenyl compounds (**b** series) have similar structures. However, in certain **b** compounds, the phenyl ipso carbon has an attractive interaction with the C(3)H or C(3)CH_2CH$_3$ proton, as clearly seen in the eq-T_{ap} conformer of *threo*-**1b** as well as in the eq-E_{-sc} form of *erythro*-**1b** and *erythro*-**3b** (Figure 5). Such a CH/π interaction[21] subtly influences the conformer of aldols in solution. For example, the $J_{\alpha,\beta}$ value of 8.8 Hz in *threo*-**1b** dictates an eq-T_{ap}/eq-T_{+sc} ratio of 85:15. The preference for the eq-T_{ap} geometry is decreased to 65:35 ($J_{\alpha,\beta}$ = 7.3 Hz) in the cyclohexyl analogue *threo*-**1a**, which lacks the CH/π stabilization. This is also the case with the cyclopentanone aldols: *threo*-**3b**, eq-T_{ap}/eq-T_{+sc} = 75:25 ($J_{\alpha,\beta}$ = 7.8 Hz), versus *threo*-**3a**, eq-T_{ap}/eq-T_{+sc} = 50:50 ($J_{\alpha,\beta}$ = 5.4 Hz).

(24) Morrison, G. A.; Wilkinson, J. B. *J. Chem. Soc., Perkin Trans. 1* **1990**, 345−351.

Conclusion

Single crystal X-ray analysis is the only spectroscopic method to unambiguously determine the relative configurations of the cycloalkanone-based aldols **1**−**3**. The structural assignment using NMR analysis in solution must be combined with IR spectroscopy and molecular weight measurement. The Stiles−House empirical method can be safely applied in only limited cases. The solution-phase structures are often different from the crystalline-state geometries. Many of the aldols exist as the monomer, having an intramolecular OH···O═C hydrogen bond in hydrocarbons. Some aldols, however, possess free hydroxy groups prone to form intermolecular hydrogen bonds at higher concentrations, where the dimer or higher aggregates form without significant conformational change. Skeletally unrestricted aldols tend to have a C═O/C(α)−C(*β*)-eclipsed geometry rather than a half-chair conformation. The cycloalkanone aldols normally are in an equilibrium of several conformers, where the relative importance is controlled largely by torsional strain. Their stability is further delicately affected by various intramolecular interactions, such as the gauche interactions between the C(2) and C(3) substituents in **2** and **3** and the CH/π attraction between the cycloalkanone skeleton and phenyl substituent in the **b** series compounds.

Experimental Section

General. Melting points were measured on a YANAKO micro melting point apparatus and were uncorrected. The number-average molecular weights (MW_{obs}) of the aldols were determined using a cryoscopic apparatus consisting of an inner cell with an inside diameter of 3 cm and an outer air jacket with an inside diameter of 4.5 cm, which prevents overcooling of the solution. The inner sample cell was equipped with a Beckmann thermometer and a side arm connected to the vacuum−argon line.[23] Infrared spectra were obtained on a Perkin-Elmer 2000 or Shimadzu 8100M Fourier transform spectrophotometer. Sample cells made of KBr were used. NMR spectra were recorded on a JEOL α-400 (^{1}H NMR at 400 MHz, ^{13}C NMR at 100 MHz), ECP-500 (^{1}H NMR at 500 MHz, ^{13}C NMR at 125 MHz), or ECP-800 (^{1}H NMR at 800 MHz, ^{13}C NMR at 200 MHz) spectrometer with a deuterated solvent as an internal lock. ^{1}H NMR spectra were referenced to the chemical shift of the residual proton signal of the deuterated solvent (δ 1.38 for cyclohexane-d_{12}) or tetramethylsilane (TMS) as the internal reference. ^{13}C NMR spectra were referenced to solvent signals (δ 26.4 for cyclohexane-d_{12}). All spectra are proton decoupled. ^{1}H and ^{13}C resonances are reported in units of ppm downfield from TMS, and proton signal patterns are indicated as s, singlet; d, doublet; t, triplet; q, quartet; m, multiplet; or br, broad signal. X-ray crystallographic analyses were conducted on a Rigaku automated four-circle diffractometer AFC-7R, and the structures were solved by direct methods using the teXsan crystallographic software package from the Molecular Structure Corporation. Analytical thin-layer chromatography was performed using Merck 5715 plates precoated with silica gel 60 F254 of 0.25-mm layer thickness. The product spots were visualized with a solution of anisaldehyde. Liquid chromatographic purifications were performed by flash column chromatography, using glass columns packed with Fuji Davison silica gel BW300 (240−400 meshes).

Method of Theoretical Calculations. The gas-phase geometries of four conformers of 3-hydroxypropanal were fully optimized using the B3LYP hybrid density functional method using the 6-311++G(d,p) basis set (B3LYP/6-311++G(d,p)).[25,26] Relative energies are corrected with unscaled zero-point energy.

Preparation of Aldols. (2*R**)-2-[(*R**)-Cyclohexyl(hydroxy)methyl]cyclohexanone (*threo*-**1a**) was prepared in 92% yield by reaction of lithium enolate, generated from 1-(trimethylsiloxy)cyclohexene (1.5 g, 8.8 mmol) and *n*-butyllithium (5.5 mL of a 1.6 M hexane solution, 8.8 mmol) in THF, and cyclohexanecarbaldehyde (1.0 g, 8.8 mmol) at −78 °C for 5 min followed by the standard workup and purification by Kugelrohr distillation (120 °C at 0.2 mmHg).[16] (2*R**)-2-[(*S**)-Cyclohexyl(hydroxy)methyl]cyclohexanone (*erythro*-**1a**) was synthesized by reaction of 1-(trimethylsiloxy)cyclohexene (1.8 g, 1.0 mmol) and cyclohexanecarbaldehyde (1.1 g, 1.0 mmol) in the presence of tetrabutylammonium fluoride (1.0 mL of a 1.0 M THF solution, 1.0 mmol) in THF at −78 °C for 5 min.[17] After workup, the crude products were purified by silica gel column chromatography (70 g; eluent, 10:1 hexane−ethyl acetate mixture), followed by recrystallization from hexane to give *erythro*-**1a** in 37% yield. The physical properties were consistent with the reported ones.[27] A 1:2 mixture of (2*R**)-2-[(*R**)-hydroxy(phenyl)methyl]cyclohexanone (*threo*-**1b**) and (2*R**)-2-[(*S**)-hydroxy(phenyl)methyl]cyclohexanone (*erythro*-**1b**) was obtained by reaction of cyclohexanone (5.0 mL, 50 mmol) and benzaldehyde (5.0 mL, 50 mmol) in a 0.2 M aq NaOH solution (55 mL) at 23 °C for 24 h.[18] Purification on silica gel column chromatography (500 g; eluent, 10:1 to 7:1 hexane−ethyl acetate mixture) afforded *threo*-**1b** (1.3 g, 13% yield) and *erythro*-**1b** (2.7 g, 26% yield), whose physical properties were consistent with those reported previously.[10] Cu(I)-catalyzed 1,4-addition of diethylzinc to 2-cyclohexenone[19] was applied to the synthesis of 3-ethyl-cycloalkanone aldols, (2*R**,3*R**)-2-[(*R**)-cyclohexyl(hydroxy)methyl]-3-ethylcyclohexanone (*threo*-**2a**), (2*R**,3*R**)-3-ethyl-2-[(*R**)-hydroxy(phenyl)methyl]cyclohexanone (*threo*-**2b**), (2*R**,3*R**)-3-ethyl-2-[(*S**)-hydroxy(phenyl)methyl]cyclohexanone (*erythro*-**2b**), (2*R**,3*R**)-2-[(*R**)-cyclohexyl(hydroxy)methyl]-3-ethylcyclopentanone (*threo*-**3a**), (2*R**,3*R**)-3-ethyl-2-[(*R**)-hydroxy(phenyl)methyl]-cyclopentanone (*threo*-**3b**), and (2*R**,3*R**)-3-ethyl-2-[(*S**)-hydroxy-(phenyl)methyl]cyclopentanone (*erythro*-**3b**). The detailed procedure as well as the physical properties have been previously reported.[19] (2*R**,3*R**)-2-[(*S**)-Cyclohexyl(hydroxy)methyl]-3-ethylcyclohexanone (*erythro*-**2a**) was obtained by a modified procedure as follows. Ethylzinc enolate, generated by the Cu(I)-catalyzed 1,4-addition of diethylzinc (6.6 mL of a 4.98 M toluene solution, 33 mmol) to 2-cyclohexenone (2.9 g, 30 mmol), was cooled to −78 °C, and a boron trifluoride ether complex (4.3 g, 30 mmol) was added. After the solution was stirred for 10 min at the same temperature, cyclohexanecarbaldehyde (3.6 mL, 30 mmol) was added. The resulting solution was stirred for 6 h at the same temperature and then poured into saturated aq NH_4-Cl solution (40 mL). The usual extractive workup afforded a 1:1 mixture of *threo*-**2a** and *erythro*-**2a**. This was chromatographed on silica gel (BW 300S, 400 g; eluent, 50:100:1 hexane−dichloromethane−ethanol mixture) to give *threo*-**2a** (1.48 g, 20.7%), *erythro*-**2a** (1.36 g, 19.0%), and a threo/erythro mixture (4.31 g, 60.3%). *erythro*-**2a**: mp 77−78 °C; IR (KBr, cm^{-1}) 3415, 2927, 2855, 1692; ^{1}H NMR (400 MHz, C_6D_{12}) δ 0.90 (t, 3H, J = 7.3 Hz, C*H*$_3$), 1.99−1.48 (m, 8H), 1.51−1.58 (m, 2H), 1.60−1.67 (m, 1H), 1.70−2.22 (m, 6H), 1.90 (d, 1H, J = 7.3 Hz, O*H*), 2.08−2.16 (m, 1H), 2.22−2.38 (m, 2H), 2.41 (dd, 1H, J = 4.4 and 7.3 Hz, COC*H*CHOH), 3.72 (ddd, 1H, J = 4.4, 7.3, and 7.3 Hz, C*H*OH); ^{13}C NMR (100 MHz, $CDCl_3$) δ 11.50, 22.80, 25.05, 25.61, 25.89, 25.99, 26.31, 26.40, 30.77, 39.17, 41.06, 41.15, 59.23, 74.61, 214.56. Anal. Calcd for $C_{15}H_{26}O_2$: C, 75.58; H, 11.0. Found: C, 75.20; H, 11.38.

X-ray Diffraction Studies. Single X-ray quality crystals of *threo*-**1a**, *erythro*-**1a**, *threo*-**1b**, *erythro*-**1b**, *threo*-**2a**, *erythro*-**2a**, *threo*-**2b**, *erythro*-**2b**, *threo*-**3a**, and *erythro*-**3b** were obtained by recrystallization from ether, pentane, or hexane solution maintained at 23 or 0 °C for several days. Their mps were 28, 58−61.5, 78−79, 102−104, 68−69, 77−78, 106−108, 86−86.5, 64−67, and 84−86 °C, respectively. The

(25) Frisch, M. J.; Trucks, G. W.; Schlegel, H. B.; Scuseria, G. E.; Robb, M. A.; Cheeseman, J. R.; Zakrzewski, V. G.; Montgomery, J. A., Jr.; Stratmann, R. E.; Burant, J. C.; Dapprich, S.; Millam, J. M.; Daniels, A. D.; Kudin, K. N.; Strain, M. C.; Farkas, O.; Tomasi, J.; Barone, V.; Cossi, M.; Cammi, R.; Mennucci, B.; Pomelli, C.; Adamo, C.; Clifford, S.; Ochterski, J.; Petersson, G. A.; Ayala, P. Y.; Cui, Q.; Morokuma, K.; Malick, D. K.; Rabuck, A. D.; Raghavachari, K.; Foresman, J. B.; Cioslowski, J.; Ortiz, J. V.; Baboul, A. G.; Stefanov, B. B.; Liu, G.; Liashenko, A.; Piskorz, P.; Komaromi, I.; Gomperts, R.; Martin, R. L.; Fox, D. J.; Keith, T.; Al-Laham, M. A.; Peng, C. Y.; Nanayakkara, A.; Challacombe, M.; Gill, P. M. W.; Johnson, B.; Chen, W.; Wong, M. W.; Andres, J. L.; Gonzalez, C.; Head-Gordon, M.; Replogle, E. S.; Pople, J. A. *Gaussian 98*, revision A.9; Gaussian, Inc.: Pittsburgh, PA, 1998.

(26) Lee, C.; Yang, W.; Parr, R. G. *Phys. Rev.* **1988**, *B37*, 785−789. Becke, A. D. *J. Chem. Phys.* **1993**, *98*, 5648−5652.

(27) Denmark, S. E.; Stavenger, R. A.; Wong, K.-T.; Su, X. *J. Am. Chem. Soc.* **1999**, *121*, 4982−4991.

oily *threo*-**3b** was converted to the *p*-bromobenzoate derivative (pyridine, 25 °C, 12 h), whose crystals were obtained by recrystallization from hexane at 25 °C, mp 90−91 °C. The X-ray irradiation to the aldol crystals except for *threo*-**1a** were conducted at 25 °C with graphite-monochromated Cu Kα. For *threo*-**1a**, the diffraction data were corrected at 0 °C. The orientation matrix and best cell dimensions were calculated by using 22−25 carefully centered reflections. The assigned crystal system and space group were uniquely determined by systematic absences in the diffraction data. Intensities of three standard reflections were recorded after every 150 reflections. Carbon, oxygen, hydroxy hydrogen, and some other hydrogen atoms were found in the difference electron density maps. All non-hydrogen atoms were anisotropically refined. The remaining hydrogen atoms were calculated and treated as idealized riding model contributions. For *threo*-**1a**, *threo*-**1b**, *erythro*-**2a**, *threo*-**2b**, *threo*-**3a**, and *erythro*-**3b**, no absorption correction was applied. Final difference electron density maps showed no features outside the range from 0.12 to −0.18 eÅ^{-3}, from 0.14 to −0.13 eÅ^{-3}, from 0.09 to −0.14 eÅ^{-3}, from 0.18 to −0.21 eÅ^{-3}, from 0.13 to −0.13 eÅ^{-3}, and from 0.22 to −0.20 eÅ^{-3}, respectively. An empirical absorption correction based on an azimuthal scan of several reflections was applied for *erythro*-**1a**, *erythro*-**1b**, *threo*-**2a**, *erythro*-**2b**, and the *p*-bromobenzoate derivative of *threo*-**3b**, whose transmission factors ranged from 0.77 to 1.00, 0.67 to 1.00, 0.69 to 1.00, 0.45 to 1.00, and 0.45 to 1.00, respectively. In each case, the final difference electron density maps showed no features outside the range from 0.25 to −0.39 eÅ^{-3}, from 0.15 to −0.20 eÅ^{-3}, from 0.25 to −0.25 eÅ^{-3}, from 0.18 to −0.21 eÅ^{-3}, and from 0.18 to −0.20 eÅ^{-3}. The crystallographic data are listed in Table 1 for all the crystalline aldols and the *p*-bromobenzoate of *threo*-**3b**.

Molecular Weight Determination. Cryoscopic measurement was used to determine the aldol molecular weight averages. The procedures are the same as those described previously.[23] The molecular weights were calculated using the equation $\Delta T = K_f\omega/MW_{obs}$ (ΔT = freezing point depression (deg), K_f = molar depression of the solvent, ω = weight (g) of solute in 1000 g of solvent, and MW_{obs} = number-average molecular weight). The K_f values of benzene and cyclohexane were calculated to be 5.16 and 22.3 on the basis of the depression of a benzene (10.53 g) solution and a cyclohexane (10.13 g) solution by naphthalene (118.6−566.6 mg and 17.0−67.6 mg, respectively). The experimental parameters are listed below in the order of sample (g), solvent (mL), concentration (ω), ΔT, and MW_{obs}. *threo*-**1a** (274.5 mg): benzene (13 mL); 100 mM (ω = 24.2); ΔT 0.65, 0.62, 0.62; MW_{obs} 192, 201, 201. *threo*-**1a** (548.9 mg): benzene (13 mL); 200 mM (ω = 48.3); ΔT 1.22, 1.11, 1.09; MW_{obs} 204, 225, 229. *threo*-**1a** (823.4 mg): benzene (13 mL); 300 mM (ω = 72.5); ΔT 1.69, 1.63, 1.66; MW_{obs} 221, 229, 226. *threo*-**1a** (35.5 mg): cyclohexane (13 mL); 13 mM (ω = 3.51); ΔT 0.31, 0.31, 0.31; MW_{obs} 253, 253, 253. *erythro*-**1a** (273.4 mg): benzene (13 mL); 100 mM (ω = 24.1); ΔT 0.55, 0.56, 0.56; MW_{obs} 226, 222, 222. *erythro*-**1a** (546.8 mg): benzene (13 mL); 200 mM (ω = 48.1); ΔT 1.09, 1.08, 1.09; MW_{obs} 228, 230, 228. *erythro*-**1a** (820.2 mg): benzene (13 mL); 300 mM (ω = 72.2); ΔT 1.67, 1.65, 1.66; MW_{obs} 223, 226, 224. *erythro*-**1a** (35.5 mg): cyclohexane (13 mL); 13 mM (ω = 3.51); ΔT 0.32, 0.32, 0.30; MW_{obs} 245, 245, 261. *threo*-**1b** (263.8 mg): benzene (13 mL); 100 mM (ω = 23.2); ΔT 0.53, 0.57, 0.53; MW_{obs} 226, 210, 226. *threo*-**1b** (527.8 mg): benzene (13 mL); 200 mM (ω = 46.5); ΔT 0.99, 1.01, 1.04; MW_{obs} 242, 238, 230. *threo*-**1b** (791.7 mg): benzene (13 mL); 300 mM (ω = 69.8); ΔT 1.56, 1.66, 1.61; MW_{obs} 230, 217, 223. *threo*-**1b** (34.4 mg): cyclohexane (13 mL); 13 mM (ω = 3.37); ΔT 0.33, 0.33, 0.34; MW_{obs} 230, 230, 223. *erythro*-**1b** (263.8 mg): benzene (13 mL); 100 mM (ω = 23.2); ΔT 0.62, 0.57, 0.63; MW_{obs} 193, 210, 190. *erythro*-**1b** (527.8 mg): benzene (13 mL); 200 mM (ω = 46.5); ΔT 1.06, 1.05, 1.05; MW_{obs} 226, 228, 228. *erythro*-**1b** (791.7 mg): benzene (13 mL); 300 mM (ω = 69.8); ΔT 1.49, 1.48, 1.49; MW_{obs} 241, 243, 241. *erythro*-**1b** (34.2 mg): cyclohexane (13 mL); 13 mM (ω = 3.38); ΔT 0.39, 0.35, 0.35; MW_{obs} 193, 215, 215. *threo*-**2a** (309.5 mg): benzene (13 mL); 100 mM (ω = 27.2); ΔT 0.54, 0.57, 0.52; MW_{obs} 260, 247, 270. *threo*-**2a** (930.0 mg): benzene (13 mL); 300 mM (ω = 81.9); ΔT 1.52, 1.54, 1.50; MW_{obs} 278, 274, 282. *threo*-**2a** (1550.2 mg): benzene (13 mL); 500 mM (ω = 136.4); ΔT 2.42, 2.39, 2.38; MW_{obs} 291, 295, 296. *threo*-**2a** (40.0 mg): cyclohexane (13 mL); 13 mM (ω = 3.95); ΔT 0.34, 0.35, 0.36; MW_{obs} 259, 252, 245. *erythro*-**2a** (309.3 mg): benzene (13 mL); 100 mM (ω = 27.2); ΔT 0.57, 0.55, 0.55; MW_{obs} 246, 255, 255. *erythro*-**2a** (929.5 mg): benzene (13 mL); 300 mM (ω = 81.8); ΔT 1.40, 1.39, 1.37; MW_{obs} 302, 304, 308. *erythro*-**2a** (1551.0 mg): benzene (13 mL); 500 mM (ω = 136.5); ΔT 2.05, 2.05, 2.00; MW_{obs} 344, 344, 352. *erythro*-**2a** (40.6 mg): cyclohexane (13 mL); 13 mM (ω = 3.95); ΔT 0.33, 0.30, 0.31; MW_{obs} 271, 298, 288. *threo*-**2b** (302.6 mg): benzene (13 mL); 100 mM (ω = 26.6); ΔT 0.58, 0.57, 0.57; MW_{obs} 237, 241, 241. *threo*-**2b** (906.7 mg): benzene (13 mL); 300 mM (ω = 79.8); ΔT 1.24, 1.21, 1.23; MW_{obs} 332, 340, 335. *threo*-**2b** (1510.2 mg): benzene (13 mL); 500 mM (ω = 132.9); ΔT 1.81, 1.79, 1.78; MW_{obs} 379, 383, 385. *threo*-**2b** (50.0 mg): cyclohexane (20 mL); 11 mM (ω = 3.21); ΔT 0.21, 0.19, 0.19; MW_{obs} 341, 377, 377. *erythro*-**2b** (302.2 mg): benzene (13 mL); 100 mM (ω = 26.6); ΔT 0.55, 0.55, 0.56; MW_{obs} 250, 250, 245. *erythro*-**2b** (906.7 mg): benzene (13 mL); 300 mM (ω = 79.8); ΔT 1.33, 1.36, 1.33; MW_{obs} 310, 303, 310. *erythro*-**2b** (1511.1 mg): benzene (13 mL); 500 mM (ω = 133.0); ΔT 2.02, 2.00, 1.99; MW_{obs} 340, 343, 345. *erythro*-**2b** (29.0 mg): cyclohexane (13 mL); 10 mM (ω = 2.86); ΔT 0.16, 0.14, 0.14; MW_{obs} 399, 456, 456. *threo*-**3a** (38.0 mg): cyclohexane (13 mL); 13 mM (ω = 3.75); ΔT 0.34, 0.34, 0.36; MW_{obs} 246, 246, 232. *threo*-**3b** (38.0 mg): cyclohexane (13 mL); 13 mM (ω = 3.75); ΔT 0.32, 0.35, 0.34; MW_{obs} 261, 239, 246.

Acknowledgment. This work was supported by a Grant-in-Aid for COE Research (No. 07CE2004) from the Ministry of Education, Culture, Sports, Science and Technology, Japan. Authors thank Mr. T. Noda for making the cryoscopic measurement apparatus.

Supporting Information Available: ORTEP drawings with numbering schemes, tables of atomic parameters, anisotropic temperature factors, and complete listings of bond angles and interatomic distances for *threo*-**1a**, *erythro*-**1a**, *threo*-**1b**, *erythro*-**1b**, *threo*-**2a**, *erythro*-**2a**, *threo*-**2b**, *erythro*-**2b**, *threo*-**3a**, *erythro*-**3b**, and the *p*-bromobenzoate derivative of *threo*-**3b** as well as the result of DFT calculations for 3-hydroxypropanal (51 Pages). This material is available free of charge via the Internet at http://pubs.acs.org.

JA0110978